J. of the Korean Radioactive Waste Society
Vol.8(3), P. 181-188, Sept. 2010.

Decontamination Characteristics of 304 Stainless Steel Surfaces by a Q-switched Nd:YAG Laser at 532 nm

532 nm 파장의 큐스위치 Nd:YAG 레이저를 이용한 스테인리스 스틸 표면 제염특성

Jei-Kwon Moon[1], Byambatseren Baigalmaa, Hui-Jun Won and Kune-Woo Lee
Korea Atomic Energy Research Institute, 1045 Daedeok-daero Yuseong-gu, Daejeon

문제권[1], 바이갈마, 원휘준, 이근우
한국원자력연구원, 대전시 유성구 대덕대로 1045

(Received July 16, 2010 / Revised August 13, 2010 / Approved September 06, 2010)

Abstract

Metal surface decontamination characteristics were investigated by using a laser ablation method. A second harmonic generation of a Q-switched Nd:YAG laser with a wave length of 532 nm, a pulse energy of 150 mJ and a pulse width of 5 ns was employed to assess the decontamination performance for metal surfaces contaminated with $CsNO_3$, $Co(NH_4)_2(SO_4)_2$, Eu_2O_3 and CeO_2. The ablation behavior was investigated for the decontamination variables such as a number of laser shots, laser fluence and an irradiation angle. Their optimum values were found to be 8, 13.3 J/cm^2 and 30°, respectively. The decontamination efficiency was different depending on the kinds of the contaminated ions, due to their different melting and boiling points and was in the order: $CsNO_3$>$Co(NH_4)_2(SO_4)_2$>Eu_2O_3>CeO_2. We also evaluated a correlation between the metal ablation thickness and the number of laser shots for the different laser fluences.

Key words : Ablation decontamination, Q-switched Nd:YAG laser, Second harmonic generation, High radioactive facilities, Radioactive metal waste

요 약

레이저 용발법에 의한 금속 표면 제염특성을 평가하였다. 레이저로는 파장 532 nm, 펄스에너지 150 mJ, 펄스폭 5 ns의 큐스위치 Nd:YAG 를 적용하였고, 금속 표면에 $CsNO_3$, $Co(NH_4)_2(SO_4)_2$, Eu_2O_3 그리고 CeO_2 를 오염시켜 이들의 제염 특성을 평가하였다. 제염 변수로는 레이저 적용횟수, 레이저 에너지 밀도 및 레이저 조사 각도 특성을 평가하였으며 각각 8, 13.3 J/cm^2 및 30°의 최적 조건을 확인하였다. 제염 효율은 오염성분의 비점과 관련이 있었으며 $CsNO_3$〉$Co(NH_4)_2(SO_4)_2$〉Eu_2O_3〉CeO_2 순이었다. 또한 여러 에너지 밀도 조건에서 스테인레스 스틸 재질의 식각 깊이 제어 특성을 규명하였다.

중심단어 : 용발 제염, 큐스위치 Nd:YAG 레이저, 2차 하모닉스, 고방사성 시설, 방사성 금속 폐기물

1) Corresponding Author. E-mail : njkmoon@kaeri.re.kr

I. Introduction

A laser ablation decontamination technology which is reportedly a new and innovative technology has been developed to secure an appropriate decontamination technology for a refurbishment or a decommissioning of radioactive hot cells in Korea. The existing decontamination methods [1,2] such as chemical process using organic solvent or inorganic acid and physical method using blasting or brushing generate voluminous and hard manageable secondary wastes due to chemicals and abrasives. Laser decontamination technology has the characterizing advantages such as very high decontamination efficiency and very low secondary waste generation, even though it has some disadvantages such as a more or less high initial equipment cost and a little bit slow decontamination speed. Moreover, it is suitable for a decontamination of highly radioactive facilities since it is be operable in a remote control mode, thereby easily ensuring a higher safety against worker's radiational exposure. There are various industrial application of lasers depending on the types of laser sources such as solid, liquid and gas [3]. Among them, an eximer, a CO_2 and a Nd:YAG laser are reportedly applicable to an etching or ablation of materials. A CO_2 laser which has a long wave length of about 10 micro meter, meaning that it is inappropriate for a delicate processing of materials, has been used for a metal welding or cutting. Eximer laser which has a characteristic advantage of delicate processing of materials due to its short wave length of UV range, it has been importantly used for a medical surgery. However, its high equipment cost and comparatively unstable laser source problem have been impeding its extensive application to industrial purposes. On the other hand, Nd:YAG laser which has a wave length variation from IR to UV has been reviewed as the most promising for an ablation of materials due to the stability of laser source and long life time. For this reason, many researchers have been developing laser ablation technologies for an application to decontamination and cleaning. L. Li et al.[4] investigated the potential role of high power lasers in nuclear decommissioning and they reported that lasers have been being recognized as attractive decontamination tools in the nuclear industry. Thoman et al.[5] had studied the effect of laser processing parameters on the chemical and structural modifications of iron surfaces. They used a Nd:YAG laser with pulse duration of 5 ns at 355, 532 and 1064 nm, respectively and KrF excimer laser system with pulse duration of 26 ns at 248 nm. From the test results, they reported that some differences were observed in the kinds of oxides detected: FeO is mainly formed with the KrF laser whereas Fe_3O_4 is more efficiently formed in the case of the Nd:YAG laser. Tam et al.[6] reported laser cleaning techniques for the removal of surface particulates. They concluded that the main parameters which affected the cleaning process were laser fluence, pulse duration and a wavelength. Dimogerontakis et al.[7] investigated a thermal oxidation induced during a laser cleaning of an aluminum-magnesium alloy by using a Q-switched Nd:YAG laser with a pulse duration of 10 ns, and a wavelength of 1,064 nm. For the surface analyses of the treated samples, they used a X-ray photoelectron spectroscopy (XPS) and a secondary ion mass spectroscopy. It was found that a thermal oxidation took place on the alloy during the irradiation in air with a laser energy range from 0.6 to 1.4 J/cm^2. On the other hand, XRD and SEM analysis of laser irradiated cadmium were performed by the other authors[8]. They used a pulsed Nd:YAG laser (10 mJ, 12 ns, 1064 nm) and reported that the hydrodynamic effects were apparent with a liquid flow which formed a recast material around the periphery of the laser focal area. Cabalin et al.[9] carried out the study on the laser ablation of stainless steel in air at atmospheric pressure. They reported that the laser ablation efficiency depends on a number of experimental parameters including laser characteristics, material properties (optical and thermal), sample surface conditions, sampling geometry, kinds of gas and pressure of the surrounding gas. In our previous study[10], we investigated the

effect of NO_3^- and OH^- ions on the laser ablation of Cs^+ ion on type 304 stainless steel using a Q-switched Nd:YAG with a wave length of 1,064nm. We found that the decontamination efficiency could be improved by the pretreatment with KNO_3 solution.

In the present study, we investigated the basic performance of a Q-switched Nd:YAG laser system with a second harmonic generation (532nm) for the decontamination of the type 304 stainless steel surrogate specimens contaminated with cesium and cobalt ions, europium oxide and cerium oxide, respectively.

II. Experimental

1. Specimen preparation and analysis

Type 304 stainless steels were cut in a rectangular form for experimental specimens. They are polished with abrasive papers and washed with water and ethyl alcohol. The four kinds of simulated specimens have been used for laser decontamination tests. The experimental specimens were prepared as follows: $Co(NH_4)_2(SO_4)_2$ and $CsNO_3$ solutions which are designated to simulate the ionic contaminations were dropped onto the specimen surfaces, respectively. On the other hand, a Eu_2O_3 and a CeO_2 powder (Aldrich Chemical Company, Inc.) diluted with distilled water, simulating particulate contaminations, were slowly dropped onto the surface of stainless steel specimen by injection. Prior to laser irradiation, the morphologies and relative atomic molar percent of the elements on the specimen were analysed by SEM-EPMA (JEOL JSM-6300). After laser irradiation, the relative atomic molar percent of the affected zone was also analyzed by the same process. One irradiated spot was magnified to fifty, one hundred and one thousand times, respectively. The three points in a spot were investigated and averaged for one data point. The content of carbon atom was excluded in the surface composition.

2. Laser Irradiation Setup

A second harmonic generation of a Q-switched Nd:YAG laser with pulse duration of 5 ns, a wave length of 532 nm, and maximum repetition rate of 10 Hz was used. All the tests were performed at pulse energy of 150 mJ. The laser was tightly focused on the target. Before transmitting the beam through the focusing lens it was shaped with the help of the configuration of a set of lenses that provide uniform temporal and spatial distribution of energy within the beam. Fig. 1 shows a schematic diagram of the experimental apparatus. Surrogate specimen was mounted on a X-Y stage. A flying articulate optics was used for a transfer and a convergence of a laser beam at the target point. The specimen was irradiated by changing the angle and the number of laser shots. The laser shot number was varied from 1 to 32 and the fluence from 7.46 to 19.23 J/cm^2. The fluence was calculated by measuring the pulse energy with a Joule meter and estimating the beam diameter.

III. Results and Discussion

1. Characterization of Samples

The morphologies and the chemical elements of the testing specimens are represented in Fig. 2 and Table 1,

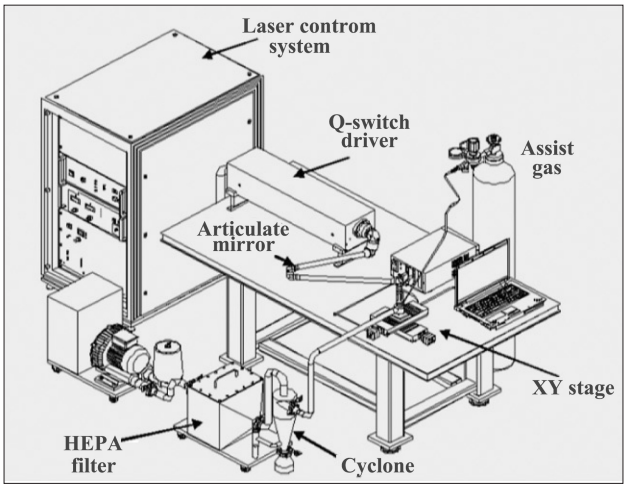

Fig. 1. Schematic diagram of the experimental setup.

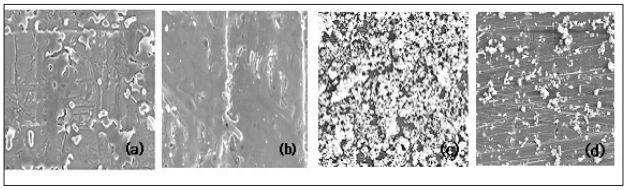

Fig. 2. SEM micrographs of stainless steel surface contaminated with (a) $CsNO_3$, (b) $Co(NH_4)_2(SO_4)_2$, (c) Eu_2O_3 and (d) CeO_2.

Table 1. Relative atomic molar ratios before laser irradiation.

Element	N	O	Ni	S	Cr	Fe	H	Eu	Cs	Ce	Co
$Co(NH_4)_2(SO_4)_2$	2.0	10.7	6.9	0.2	18	59.2	trace	-	-	-	3.0
Eu_2O_3	-	30.6	7.7	-	10.1	45.6	-	6	-	-	-
$CsNO_3$	4.5	25.4	5.9	-	13.6	45.6	-	-	5.0	-	-
CeO_2	-	11.6	6.0	-	17.1	58.3	-	-	-	7.0	-

respectively. The specimen (a) and (b) which are designated to simulate ionic contaminations show very well dispersed contamination on the surfaces, while the specimens (c) and (d) show obviously particulate contaminations. Table 1 shows that each specimen contains the chemical elements properly according to the simulation. The elements of Fe, Cr, Ni which are dominant ones for all specimens are originated from the base metal of stainless steel and the oxygen content in each sample might include the oxygen in the atmosphere.

2. Effect of laser fluence

Removal efficiency of the four contaminants on the type 304 stainless steel specimens was investigated against the laser fluence, fixing the number of laser shots at 8 and the results are given in Fig. 3. It shows that the $CsNO_3$, $Co(NH_4)_2(SO_4)_2$, Eu_2O_3 and CeO_2 are removed rapidly for the fluence increase up to about 13.3 J/cm^2 and then very slowly for a fluence increase, even though the removal efficiencies are different from the contaminating ions. The contaminants are removed continuously for a fluence increase up to about 20 J/cm^2 though. However, considering the removal efficiency slope, the laser fluence of 13.3 J/cm^2 was determined as an appropriate condition for a decontamination of the type 304 stainless steel. The laser fluence conditions for an ablation threshold are different from the kinds of laser and the ablation materials. Fukui et al.[11] reported that about 90% of cesium ion on the stainless steel was removed by the application of more than 4 laser shots at the laser fluence of 5.3 J/cm^2 in their laser decontamination study with a Q-switched Nd:YAG laser. Delaporate et al.[12] studied a decontamination of radioactive inconel specimens by using an excimer laser and reported that ablation plasma was generated for the fluence higher than 1 J/cm^2.

3. Effect of the number of laser shots

To determine the optimum laser shot numbers for a removal of $CsNO_3$, $Co(NH_4)_2(SO_4)_2$, Eu_2O_3 and CeO_2, the fractional removals were evaluated as the function of laser shot number at 13.3 J/cm^2 for the 4 kinds of specimens as shown in Fig. 4. It shows that the four ions are removed proportionally to the number of shots up to 8, even though the removal efficiency is a little bit different from the ions. The cesium ions is shown to be removed almost completely and more than 99% for cobalt ions and 98.5% for europium and cerium oxides after the first 8 shots. In the case of europium and cerium oxides, about 32 shots are required to obtain 99%

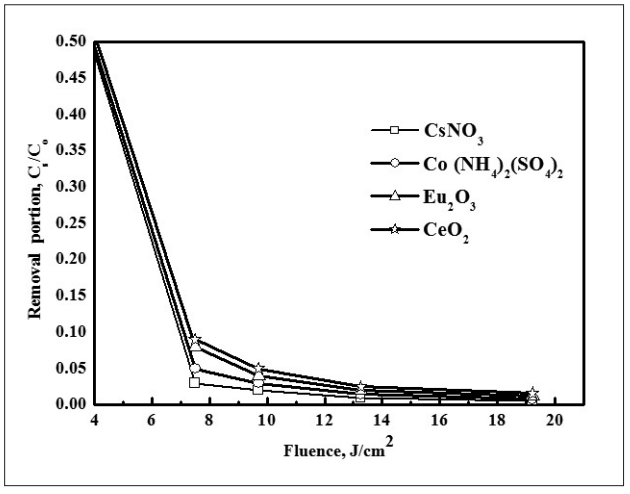

Fig. 3. Removal behavior of $CsNO_3$, $Co(NH_4)_2(SO_4)_2$, Eu_2O_3 and CeO_2 after laser against the fluence, fixing the number of laser shots at 8.

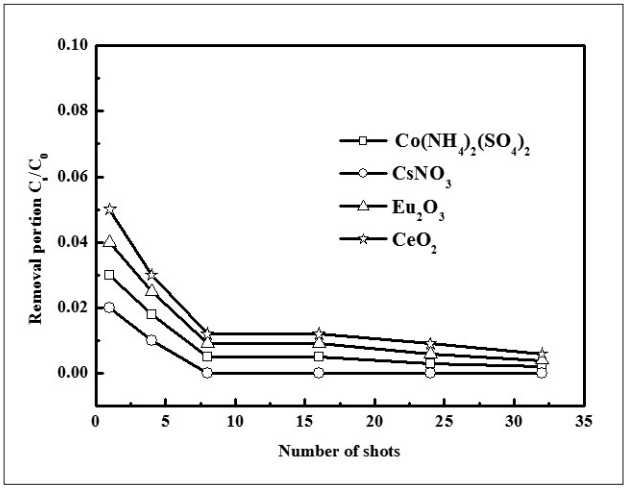

Fig. 4. Removal behavior of $CsNO_3$, $Co(NH_4)_2(SO_4)_2$, Eu_2O_3 and CeO_2 after laser against the number of laser shots. (13.3 J/cm^2 and 10 Hz).

removal efficiencies. This might be related with their different physical properties such as the melting and boiling points. The boiling point of $CsNO_3$ (849 ℃) is lower than those of cobalt ammonium sulfate (2,927 ℃), europium oxide (4,118 ℃) and cerium oxide (3,500 ℃). Considering that an ablation of material, when irradiated by a laser, is occurred sequently by melting and then boiling, these lower boiling points might affect the easy evaporation of cesium and cobalt ions compared with the europium and cerium oxides. On the other hand, in the case of europium oxide and cerium oxide, most of them are seemingly removed by the co-evaporation with the base metal of a 304 stainless steel which has a lower boiling point than the europium oxide. However, some portions still remain in the base metal as the melting phases even for further application of laser shots due to their high boiling point.

4. Surface temperature evaluation

By assuming that the ablation occurs in one dimension, the molar flux can be given by the Hertz-Knudsen equation[13] given in Eq. (1). The equation shows that the ablation flux is dependent on the vapor pressure difference between the surface saturation vapor pressure and the vapor pressure in the infinite position. Therefore, if the Ps equal to Pi, there is no evaporation at all.

$$J_i = s\frac{Ps(T)-P_i}{(2\Pi m_i k_B T)^{1/2}} \quad \cdots\cdots (1)$$

where J_i (species/cm²s) is the flux and *mi* the mass of species *i* that leaves the surface, $s \leq 1$ is a correction factor which depends on the particular mechanism of evaporation. P_s and P_i (atm) are the saturation vapor pressure and the partial pressure of molecules at infinity, respectively. T (K) is the absolute temperature and kb (1.381×10^{-23} Ws/K) is the Boltzmann constant. The saturation vapor pressure can be evaluated by the Clausius-Clapeyron equation[13] as given in Eq. (2).

$$\mathrm{Ln}\left(\frac{P_i}{P_s}\right) = -\frac{\triangle H_v}{R}\left(\frac{1}{T}-\frac{1}{T_b}\right) \quad \cdots\cdots (2)$$

where P_s is the saturation vapor pressure, $\triangle H_v$ (J/mole) is the heat of vaporization at T_b and T_b (K) is the boiling temperature of the evaporating molecule. R (8.314 J/mole K)is the gas constant.

The surface temperatures during a laser ablation for the given laser fluence conditions are calculated. First, we obtained the ablation fluxes from the experimental data for SUS and plotted against the laser application time for the two laser fluence conditions as given in Fig. 5. The slopes of the two lines correspond to the ablation fluxes for the two laser fluences of 13.3 J/cm² and 57.3 J/cm², respectively. These flux data were inserted to the Hertz-Knudsen equation to evaluate the saturation vapor pressure. Then, the obtained vapor pressure data were once again inserted to the Clasius-Clapeyron equation to evaluate the surface temperature. Thus, relation between the ablation molar flux and the surface temperatures for the two laser fluence conditions was obtained as shown in Fig. 6. It shows that the surface temperatures are 5,000 K for 13.3 J/cm² and 5,600 K for 57.3 J/cm². On the contrary, it means that if the ablation temperature is given, the ablation flux can be estimated.

5. Effect of laser irradiation angle

Fig. 7 shows the removal behavior of the contaminants on the stainless steel at various irradiation angles. The specimen was irradiated by changing position of angle at 8 laser shots. The angle of 0° means that the irradiation of laser beam is perpendicular to the specimen. The angle of

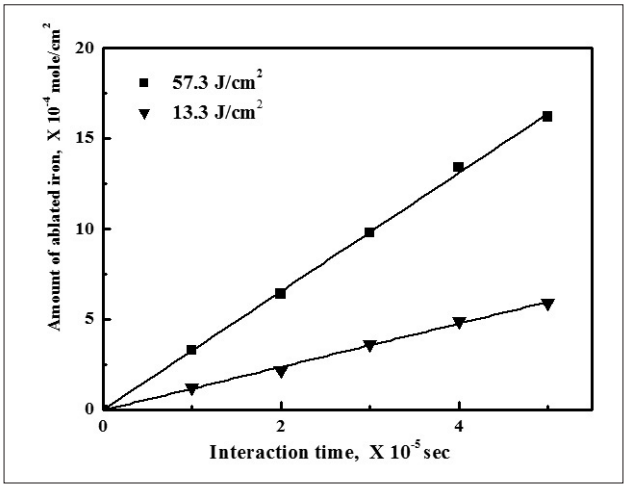

Fig. 5. Experimental ablation data of stainless steel for two laser fluences

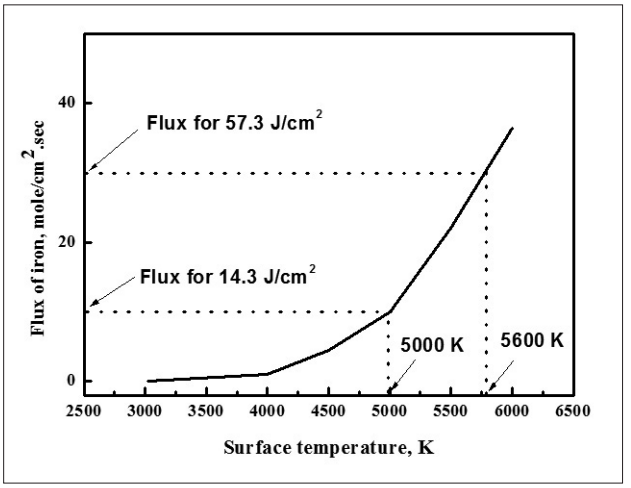

Fig. 6. Curves relating the molar ablation flux and surface temperature.

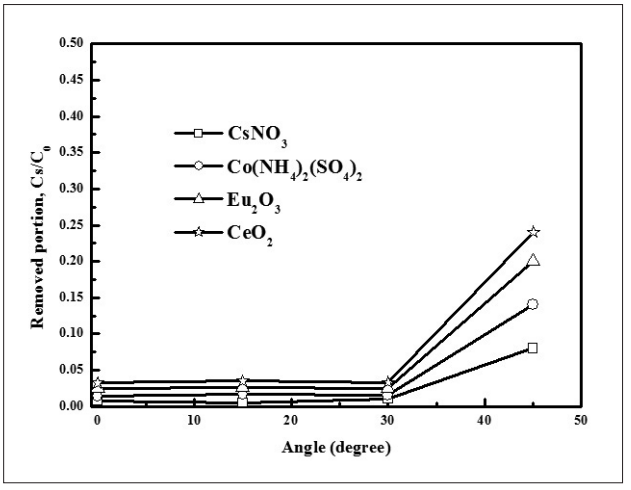

Fig. 7. Removal behavior of the contaminants for various irradiation angles (laser fluence: 13.3 J/cm²).

15° means that the specimen is inclined at fifteen degrees from the perpendicular of laser beam. It shows that the 4 kinds of specimen were effectively removed for the angle in the range between 0° and 30°. When the irradiation angle increases to 45°, however, the removal efficiency decreases suddenly. Therefore, the irradiation angles which are variable for ensuring decontamination performances were found to be in the range between 0° and 30°.

The exposed specimen morphologies were examined by SEM at a magnification of 50X. SEM micrographs of the specimens before and after the laser irradiation at the angles of 0°, 15°, 30°, 45° are shown in Fig. 8. The surface of the specimen was contaminated with (a) $CsNO_3$, (b) $Co(NH_4)_2(SO_4)_2$,(c) Eu_2O_3 and (d) CeO_2, respectively. Also the numbers of (1), (2), (3) and (4) in the photos represent the laser irradiation angles of 0°, 15°, 30° and 45°, respectively. From the SEM analysis it was found that Co^{2+}, Cs^{+} ions exist in the form of a crystal as in (a) and (b). On the other hand, the Eu_2O_3 and CeO_2 on the specimen are dissipated in a powder form as in (c) and (d), respectively. During the application of laser energy, the metal surfaces and contaminants are ablated and the craters of different shapes depending on the irradiation angles are formed as shown in (a-1,2,3,4), (b-1,2,3,4), (c-1,2,3,4) and (d-1,2,3,4). It can be seen that the circle form of crater changes to an ellipsoidal shape as the irradiation angle increases to 45° and the removal efficiency become worse. The formation of crater has already been reported by the other researchers [14]. They reported that the crater was connected with boiling process.

6. Correlation of the ablation depth and the number of laser shots

In order to evaluate the laser application conditions for required decontamination efficiency, the relation between the removal depths of 304 stainless steel and the number of laser shots for the four different laser fluences was obtained as in Fig. 9. It shows that the ablation thickness

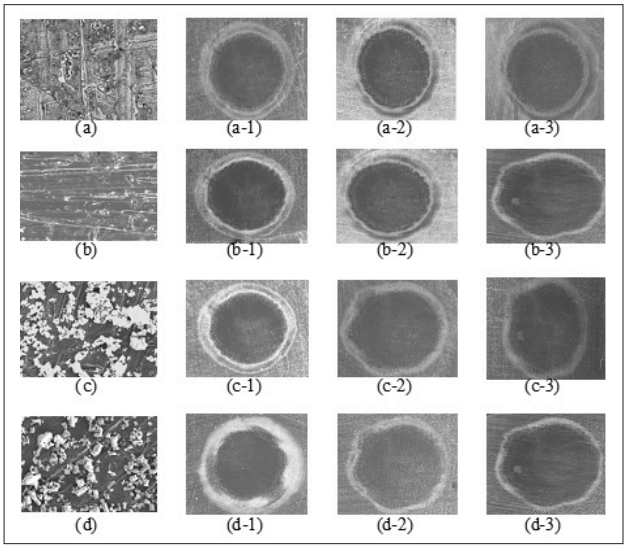

Fig. 8. SEM images of SUS 304 surface (50X) contaminated with (a) $CsNO_3$, (b) $Co(NH_4)_2(SO_4)_2$, (c) Eu_2O_3 and (d) CeO_2 before and after 8 laser shots of laser irradiation at (1) 0°, (2) 15°, (3) 30°, (4) 45°.

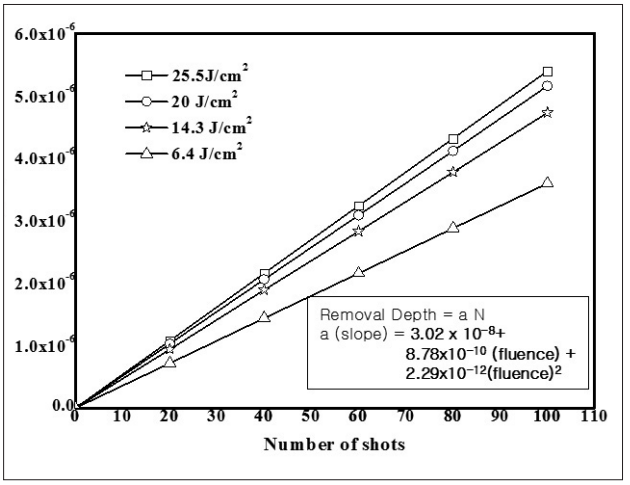

Fig. 9. Correlation of the removal depth and the number of laser shots for the different fluences.

increase linearly to the number of laser shots although the slopes are different depending on the fluences. These relations could be represented by a integrated linear equation: D = aN, where D is depth, a is slope and N is the number of shots. The equation can make it possible to determine the process conditions such as a number of laser shots and laser fluence to obtain a designated ablation thickness for a required decontamination factor.

IV. Conclusion

A second harmonic generation of a Q-switched Nd:YAG laser with a wave length of 532 nm, a pulse energy of 450 mJ, and a pulse width of 5 ns was employed to assess the decontamination performances for metal surfaces contaminated with $CsNO_3$, $Co(NH_4)_2(SO_4)_2$, Eu_2O_3 and CeO_2. We evaluated the effect of decontamination process variables such as a number of laser shots, laser fluence and an allowable irradiation angle on the ablation characteristics. Optimum values of the variables were found to be 8, 13.3 J/cm^2 and 30°, respectively. The decontamination efficiency was shown to be different depending on the kinds of the contaminated ions, which have the different melting and boiling points. The removal efficiencies for the three contaminants were in the order of $CsNO_3$> $Co(NH_4)_2(SO_4)_2$>Eu_2O_3>CeO_2. We evaluated a correlation between the metal ablation depths and the number of laser shots for the different laser fluences in order to make it possible to estimate ablation conditions such as a number of laser shots and laser fluence required for a designated decontamination factor, which can be different from the case by case.

Acknowledgments

This work has been carried out under the Nuclear R & D Program funded by Ministry of Education, Science and Technology.

Reference

[1] 양영미, 최왕규, 오원진, 유승곤, "우라늄 화합물로 오염된 금속폐기물의 전해제염" 방사성폐기물학회지, 1(1), 11 (2003).

[2] M. A. Blessa, E. B. Borghi, S. P. Ali and P. J. Morando, " Cleaning of stainless steel surfaces and oxide dissolution by malonic and oxalic acids", J. of Nuclear Materials, 229, 115 (1996).

[3] J. Meijer, "Laser beam machining (LBM), state of the art and new oppertunities", J. of materials process. Technol., 149, 2 (2004).

[4] L., Li "The potential role of high power lasers in nuclear decommissioning", Nucl. Energy 41, 397(2002).

[5] A. L. Thomann, A. B. Wegscheider, C. Boulmer-Leborgne, A. Pereira, P. Delaporate, M. Sentis and T. Sauvage, "Chemical and structural modifications of laser treated iron surfaces: investigation of laser processing parameters", Applied Surface Science 230, 350 (2004).

[6] A. C. Tam, W. P. Leung, W. Zapka and W. Ziemlich, "Laser cleaning techniques for the removal of surface particulates", J. Appl. Phys. 71, 3515 (1992).

[7] T. Dimogerontakis, R. Oltra and O. Heintz, Appl. Phys. 81, 1173 (2005).

[8] M. S. Reafique, M. T. Firdos, K. Aslam, M. S. Anwar, M. Imran, and H. Latif, Laser Physics. 17, 1138 (2007).

[9] L. M. Cabalin, D. Romero, J. M. Baena, J. J. Laserna, "Saturation effects in the laser ablation of stainless steel in air at atmospheric pressure". Fresenius J. Anal. Chem. 365, 404 (1999).

[10] B. Baigalmaa, H. J. Won, J. K. Moon, C. H. Jung and J. H. Hyun, "A comprehensive study on the laser decontamination of surfaces contaminated with Cs^+ ion", Applied Radiation and Isotopes, 67, 1526 (2009).

[11] Y. Fukui, R. Ogawa, N. Ishijima and N. Kenichi "Development of laser decontamination", JNC TN9410 99-014 (1999).

[12] Ph. Delaporate, M. Gastaud, W. Marine, M. Semtis, O. Uteza, P. Thouvenot, J. L. Alcaraz, J. M. Le Samedy and D. Blin, "Dry eximer laser cleaning applied to nuclear decontamination", Applied Surface Science 298, 208 (2003).

[13] Dieter, "Laser Processing and Chemistry", P 190, Springer, 3rd Revised and Enlarged Edition, 2000.

[14] M. S. Lafique, R. M. Khaleequr, T. Fridos, K. Aslam, A.M. Shabaz and H., Latif, "XRD and SEM analysis of a laser irradiated cadmium:, laser Physics, 17 (9), 1138 (2007).